

## **An appraisal of characteristic mechanical properties and microstructure of friction stir welding for Aluminium 6061 alloy – Silicon Carbide (SiCp) metal matrix composite**

**Ibrahim Sabry<sup>1\*</sup>, A. M. El-Kassas<sup>2</sup>**

<sup>1</sup> Department of Manufacturing Engineering and Production Technology  
Modern Academy for Engineering and Technology, P.O. Box, Cairo 11571, Cairo, Egypt.

\*Email [ibrahem.sabry@modern-academy.edu.eg](mailto:ibrahem.sabry@modern-academy.edu.eg)

Phone: +201003719980

<sup>2</sup> Department of Production Engineering and Mechanical Design, Faculty of Engineering,  
Tanta University, P.O. Box, Tanta 31512, Egypt

Email: [ahmed.elkassas@f-eng.tanta.edu.eg](mailto:ahmed.elkassas@f-eng.tanta.edu.eg)

### **ABSTRACT**

It is expected that the demand for Metal Matrix Composite (MMCs) will increase in these applications in the aerospace and automotive industries sectors, strengthened AMC has different advantages over monolithic aluminium alloy as it has characteristics between matrix metal and reinforcement particles. However, adequate joining technique, which is important for structural materials, has not been established for (MMCs) yet. Conventional fusion welding is difficult because of the irregular redistribution or reinforcement particles. Also, the reaction between reinforcement particles and aluminium matrix as weld defects such as porosity in the fusion zone make fusion welding more difficult. The aim of this work was to show friction stir welding (FSW) feasibility for entering Al 6061/5 to Al 6061/18 wt. % SiCp composites has been produced by using stir casting technique. SiCp is added as reinforcement in to Aluminium alloy (Al 6061) for preparing metal matrix composite. This method is less expensive and very effective. Different rotational speeds, 1000 and 1800 rpm and traverse speed 10 mm \ min was examined. Specimen composite plates having thick 10 mm were FS welded successfully. A high-speed steel (HSS) cylindrical instrument with conical pin form was used for FSW. The outcome revealed that the ultimate tensile strength of the welded joint (Al 6061/18 wt. %) was 195 MPa at rotation speed 1800 rpm, the outcome revealed that the ultimate tensile strength of the welded joint (Al 6061/18 wt.%) was 165 MPa at rotation speed 1000 rpm, that was very near to the composite matrix as-cast strength. The research of microstructure showed the reason for increased joint strength and microhardness. The microstructural study showed the reason (4 %) for higher joint strength and microhardness. due to Significant of SiCp close to the boundary of the dynamically recrystallized and thermo mechanically affected zone (TMAZ) was observed through rotation speed 1800 rpm. The friction stir welded ultimate tensile strength Decreases as the volume fraction increases of SiCp (18 wt.%).

**Keywords:** Friction stir welding; Aluminium matrix composites; Al 6061; microstructure; microhardness; ultimate tensile strength.

## INTRODUCTION

The use of aluminum (Al) alloys in building high strength structural parts has increased over the years most especially in the automobile, mining, mineral, aerospace and defense industries [1]. This has been driven mostly by a need to reduce energy consumption in social and industrial usage with their high strength and low weight characteristics. Aluminum reinforced structural parts have been utilized for an increasingly complex array of components in these industries [2]. MMCs are one of such reinforced materials and are made from a mixture of reinforcements (carbides, oxides and nitrides of metallic or ceramic additions) in a tough metallic matrix. Different types of reinforcements; including continuous fibers (both monofilament and multifilament), short fibers, whiskers and particulates, from 10-60% by volume [3-5] have been investigated. The percentage (%) reinforcement has a bearing on the properties together with the mode of manufacture which can vary with each type of reinforcement used. Metal Matrix Composite (MNCs) are emerging as important versatile materials due to the wide range of properties they provide. It is possible to impart the near-net-shape for particulate (MNCs) by the powder metallurgy techniques [8]. The joining of (MMCs) Their mixture of traditional fusion welding techniques is restricted, which leads to the consideration of solid-state welding procedures such as FSW [6]. The density variation in between ceramic particles and matrix phase improved in the segregation of particles [27]. In the nugget zone, the distribution of reinforcement agents is very strict to retain as opposed to that of the composite material's as-cast base metal. The matrix composite's top viscosity impedes material flow that persuades a heterogeneous dispersal of heat stresses that decreases the joint's power. The quantity of heat generated predominantly begins responses between the reinforcement stage and the aluminum alloy matrix through the standard fusion welding method, creating brittle intermetallic amalgams in the nugget region. In addition, the welded joint produced by standard fusion welding method can be traced to porosity [7–10]. Therefore, to remove this defect, it is suggested to use solid-state joining methods to weld Al-matrix composites. As a sophisticated joining method for welding aluminum matrix composite [11], friction stir welding of a solid-state friction stir welding method (FSW) has progressed. In friction stir welding as the joint occurs in solid state, there is no consolidation instigated formation in the nugget region subsequently. Therefore, all the fusion-joining process deficiencies are disappeared [12]. Some research on friction stir welding of Al-matrix composites reinforced with separate ceramic particles has been researched in contemporary years in literature [13].

Murugan et al [14] analyzed the influence of various tool pin on microscopic inspection of FS welded AA6061 reinforced with 10 wt.% TiB<sub>2</sub> and the square pin generated fine grain structure in the weld zone. Analyzes the impact of pin profiles on mechanical characteristics and finds that joints welded with a straight square pin profile have better mechanical characteristics compared to other pin profiles. Nami et al. [15] studied the effect of tool rotation speed on grain size of FS Weld AA6061 reinforced with 15 wt.% Mg<sub>2</sub>Si. The findings showed fragmentation of particles of Mg<sub>2</sub>Si and needles of Mg<sub>2</sub>Si in the stir area in the eutectic framework. As a consequence of stirring with elevated plastic strains, homogeneous distribution of Mg<sub>2</sub>Si particles was noted in the stir area. Results of the tension test stated that the joint tensile strength was optimal at rotation speed of 1120 rpm instrument and reduced as the amount of welding passes increased. The joint's hardness increased due to modification of the base composite's solidification microstructure. This study shows that

friction stir welding is a perfect option for 15 wt. percent Mg<sub>2</sub>Si composite castings of the aluminum matrix. Murugan et al [16] optimized the ultimate tensile strength (UTS) of FS welded AA6061 strengthened with (3-7wt.%) TiC particles by applying a mathematical optimization model. The FSW samples without any post-weld thermal therapy belonging to a distinct set of parameters tested showed elevated joint effectiveness (most of which ranged from 90% to 98%) with regard to the ultimate tensile strength of the base material AA6061. It was discovered from the model assessment that the pin profile of the instrument and the welding velocity have a greater impact on the strength of the tensile. The purpose of this research is to explore the impact of FSW on Al 6061/5, 10.18 wt's microstructural and mechanical conduct. Percentage of SiCp, speed and velocity of rotation. Friction stir's mechanical and metallurgical conduct welded Al 6061/5, 10,18 wt. The percentage of SiCp aluminum matrix composite differs from the manufactured alloy matrix and aluminum matrix composite to comprehend the impact of rotational speed, travel velocity and Sic particle on FSW.

## METHODS AND MATERIALS

### Materials

In this work, the manufacture of Al 6061/Sic Aluminum Matrix Composite and Friction Stir Welding Al 6061 al-alloy reinforced with Sic particles was used to produce composite aluminum matrix. The matrix is an aluminum alloy standard Al 6061 with the official chemical composition as shown in Table 1. Silicon carbide (SiCp) reinforced Al 6061 matrix composites were produced using stir casting method as stated in the literature [17] in a top loading electrical resistance muffle furnace. SiCp average size was 400 mesh (40  $\mu$ m). Castings were generated by reinforcing Sic particles (5 and 15 wt. %). For friction stir welding, composite cut samples of the size (150 mm X750 mm X 10 mm) mm were prepared, washed and then welded along the joint line. Using the specially constructed fixture as shown in Figure 2 to clamp the welding plates, the welding studies were carried out on an automated vertical milling machine. The most important element in FSW to prevent the lifting of the plates to be welded during the welding phase and to verify coherent temperature distribution across the sample plates is the appropriate fixture design with backing plates [18]. The welding variables were adapted to generate defect-free welds based on visual inspection. Welding tests were conducted at 1000 and 18000 rpm tool rotational speed and 10 mm \min tool transverse speed. The dimensional instrument produced is shown in Figure 1(b) and Table 2. Figure 3 shows the perspective of the successful friction stir welded aluminum composite matrix plate. The observed defective friction stir welded samples were dismissed and further mechanical and microstructural characteristics were subjected. Mechanical and microstructural assessment was performed on the defect-free welded plates.

Table 1. Chemical composition of 6061 Al-alloy.

Element	Mg	Si	Fe	Cu	Mn	Zn	Cr	Ti	Al
wt. %	1.1	0.55	0.4	0.10	0.9	0.25	0.04	0.12	Remainder

Table 2. Geometrical dimensions of the friction stir welding tool.

Factors	Tool length	Pin length	Pin diameter (tip)	Pin diameter (near shoulder)	Shoulder diameter
Dimensions	67	10	1	2	30

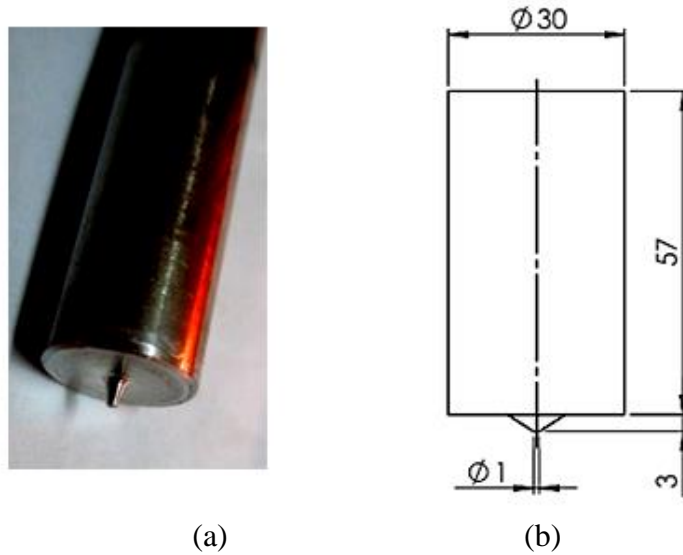


Figure 1. (a) Friction stir welding tool with a conical pin profile and (b) Tool dimensions (scale 2:1).

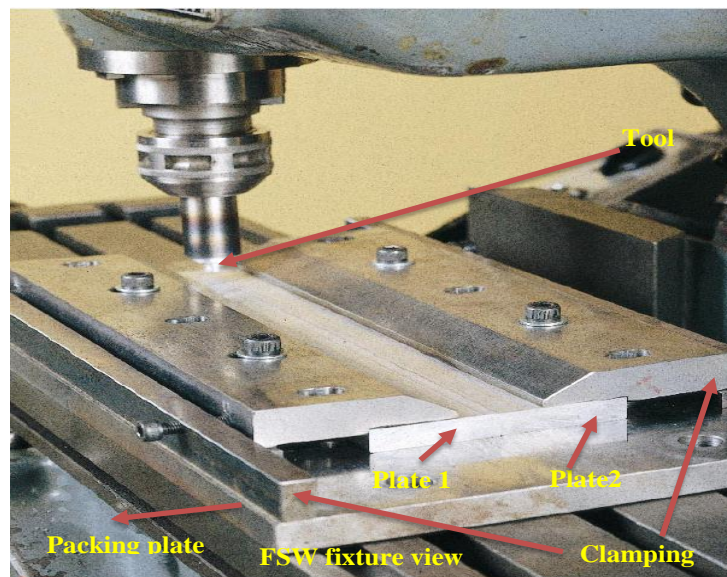


Figure 2. View of friction stir welding fixture.

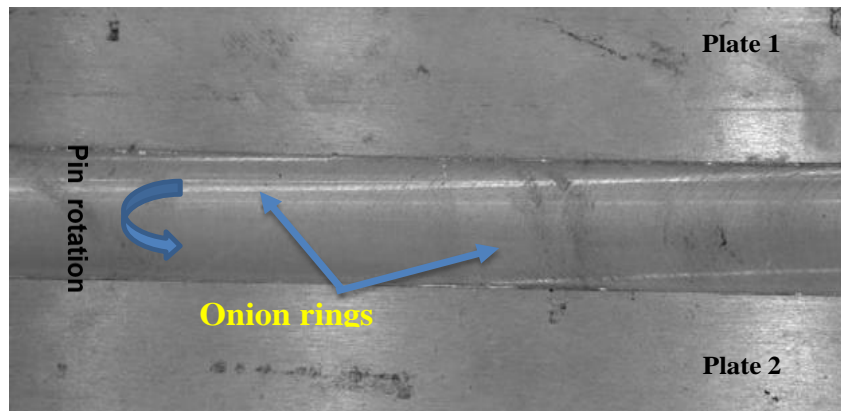


Figure 3. Friction stir welded 6061/18% SiC aluminium matrix composite (scale 2:1).

### **Material Characterization and Testing**

The metallographic samples were prepared from Al 6061 aluminum matrix composite and as welded Al 6061 aluminum matrix composites in accordance with the conventional metallographic operation followed by mirror polishing and Keller reagent etching (HCL + HF + HNO<sub>3</sub> + distilled water). The normal tensile specimen was slashed perpendicular to the joint line and prepared from all the samples in accordance with the ASTM E8-04 standard [19]. The tensile specimens were prepared 57.2 mm long, 12.2 mm wide, and 10 mm thick. The tensile tests were performed on a blue star universal tensile testing machine (SE UTE 200) with a maximum capacity of up to 200KN. The FS welded specimen's microstructure was evaluated using a china-made optical scanning microscope (XPZ-830 T). Stir cast Al-matrix microstructural assessment was also performed in the same way as cast aluminum matrix composite and welded joint. The FS welded and other samples (as cast matrix alloy and composite) microhardness examination was carried out using FIE model VM50 Vickers microhardness tester. The hardness measurements were conducted for a dwelling moment of 17 seconds at different places on both sides of the weld region at a steady load of 0.08kgf. The measurements of hardness were then defined as microhardness on average.

## **RESULTS AND DISCUSSION**

### **Visual Test**

Inspection of the upper surface of welded sample showed uniform semicircular surface ripples, occasioned by the final sweep of the trailing edge of rotating tool shoulder over weld nugget, under the influence of probe on top of pressure as shown in Figure 4. The presence of such surface ripples, known as onion rings, has been previously observed through FSW of some other alloys. The lower surface of weldments showed visually a uniform homogenous sound flat surface.

No evidence of cracking was found within the cross-sectional view of the welds as observed by optical microscopy at X200. However, visual inspection easily revealed that the crown side (top side) of the welds was quite coarse. In comparison with monolithic alloys, the crown side of a typical FSW in an Al alloy has a highly polished, machined appearance. The welds performed with AMC material consistently gave the

crownside a unique appearance that is reminiscent of what one would expect to see for a typical surface of concrete. This coarse appearance was caused by the fact that the SiCp did not adhere well with the Al at the surface of the weld adjacent to the tool shoulder.

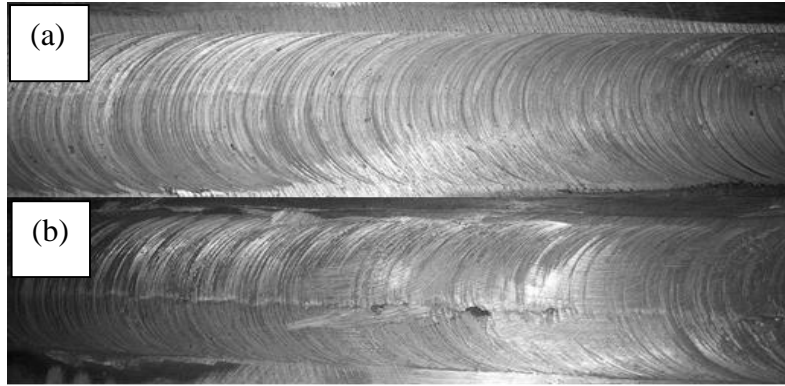


Figure 4. Welding specimen showed leading and trailing edge (a) 6061/18% SiCp at 1800 rpm (b) 6061/18% SiCp at 1000 rpm.

### Microscopic Observation of the friction stir Welded Joint

In Figure 5 the macro-structural inspection of FS welded Al 6061/18 wt. % SiCp composite plate is depicted. The macro-structural study of the welded joint revealed the continual flow of plasticized material from the advancing side (AS) to retreating side (RS). Because the thermo-mechanically impacted area was split into three: the area near the thermo-mechanically impacted area where coarse " precipitates were observed; the center zone. The size of precipitates in the heat-affected area was lower than those in the base metal area. No defects were spotted in the macrograph for the welded joint [20]. The stir zone (SZ) in this study was observed with a basin structure as reported by others [27]. The different sections of the welded joint such as weld zone (WZ), heat affected zone (HAZ), thermomechanical affected zone (TMAZ) and base metal (BM) are clearly identified in the macrograph as shown in Figure 4 [21]. The weld zone and TMAZ are characterized by adjoining regions. TMAZ is that region which experienced high thermal cycles and subjected to plastic deformation under the action of thermal cycles. WZ and TMAZ borderline have been characterized by the appearance of small-sized Sic reinforcing agents in the WZ produced due to the stirring tool action. Similar examinations have been investigated in the literature [15].

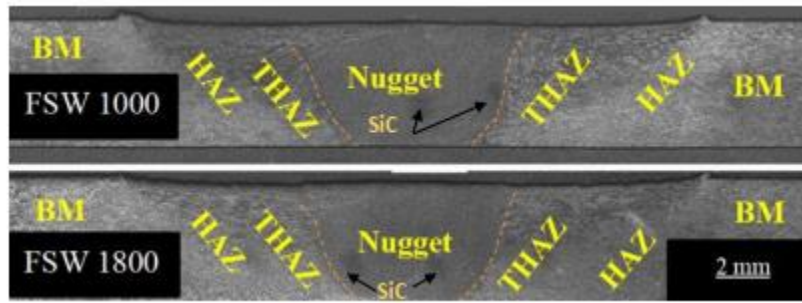


Figure 5. Macrostructure of friction stir welded for 6061 / 18% SiC composite (at 100X).

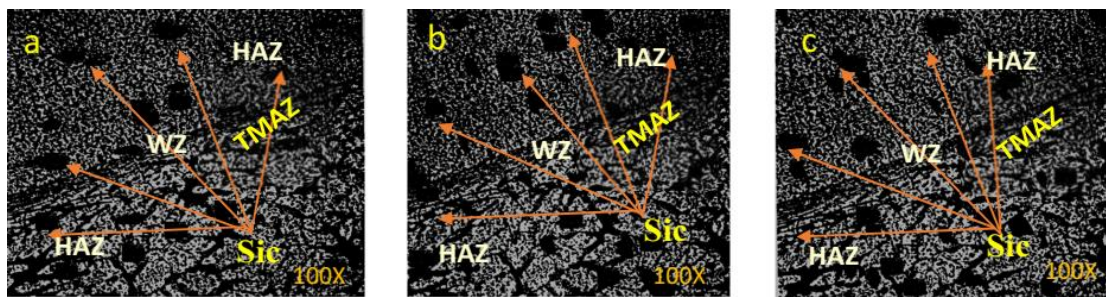


Figure 6. Optical microscopic pictures of friction stir welding for composite material at speed 1000 rpm and feed 10 mm/min (a) 6061/5% SiC (b) 6061/10% SiC (c) 6061/18% SiC

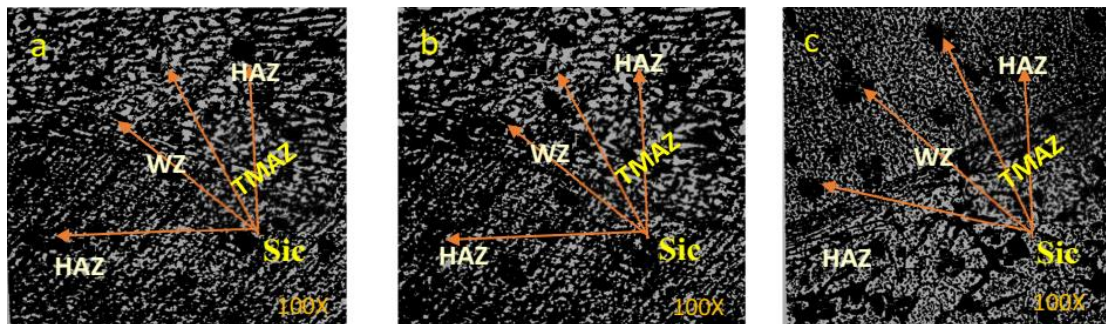


Figure 7. Optical microscopic pictures of friction stir welding for composite material at speed 1800 rpm and feed 10 mm/min. (a) 6061/5% SiC (b) 6061/10% SiC (c) 6061/18% SiC

Optical microscope pictures of weld zone as depicted in Figure 6 and Figure 6 respectively confirmed that in the weld zone no segregation of particles has been observed as reported in case of conventional fusion welding processes of aluminum matrix composite. The chances of micro porosities associated with the stir cast composite matrix were eliminated following to FSW as noticed in the optical microscope images in the weld region. A homogeneous distribution of SiC agents has been noticed in the

weld zone.

The size and distribution of precipitates in Figure 6 and Figure 7 reflects the presence of three distinct zones. At the weld centerline the precipitates are less dense and a relatively fine, whereas at the base metal they are relatively coarse and denser. It is worth to be noted that, the coarse particles were swept away at the boundary flow layers. The lower density of precipitates at weld centerline could be due to dissolution of precipitates during heating, where the temperature exceeded  $0.8T_m$  [22], and reprecipitation during relatively rapid cooling. Significant reorientation of SiCp near the dynamically recrystallized and TMAZ border has been noted. In the dynamically recrystallized area, the tiny hardening was ascribed to the existence of dislocation tangles between SiCp. The rotational movements of stir probe may affect the size of precipitates through fragmentation and dissolution processes.

### **Microhardness Inspection of the Welded Joint**

Microhardness measurement was taken across the crown side of the weld zone as shown in Figure 8 the hardness profiles for friction stir welding specimens at 10 mm/min-traverse speed, and at different rotational speeds of 1000 rpm and 1800 rpm. The hardness profiles were taken at three different locations across the weld nugget, i.e. near the weld-face, at midway through the weld nugget, and near the root of the friction stir welding joint. The weld nugget regions show in 5% SiC to 18% SiCp the higher value of hardness due to the existence of finer SiCp as well as grain refinement of the Al-matrix. The stirring action of the tool pin wears the surface of SiCp agents and reduction in the size of SiCp agents occurs. The existence of such numerous fragmented small and rounded up SiCp agents with refinement in Al-matrix remarkably enhanced the hardness of the weldments. Hardening of the composite matrix following to FSW also significantly increased the hardness in the weld zone [23]. A slight decrease in microhardness value in the thermomechanical affected zone on both sides of the weld section (i.e. advancing and retreating sides) adjacent to the WZ was noticed. The decrease in hardness in this region is ascribed to the second phase particle dissolution and coarsening prompted by thermo-mechanical conditions. It is observed that the HAZ adjacent to TMAZ on the advancing and retreating side found a gradual decrease in hardness value as compared to the TMAZ. This may be ascribed to the annealing process that takes place in the HAZ [24].

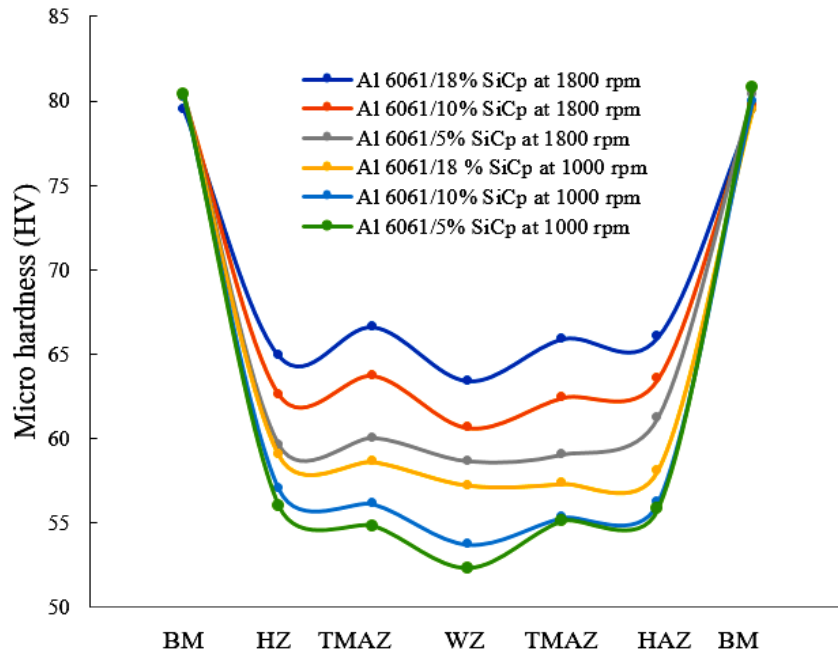


Figure 8. Microhardness across the welded joint 6061 and base metal 6061 at addition different SiCp %.

### **Tensile Behavior of the Welded Joint**

In Figure 9 introduces the stress-strain relationship acquired for all combinations of parameters by conducting a tensile test on joints. From all the observations, the tensile strength of all joints was observed to be lower than the Al 6061(BM). For steady travel speed, the tensile strength is proportional to the rotation velocity within the experimented range (1000 rpm and 1800 rpm).

In Figure 8(b) the tensile behavior of Al 6061 composite matrix and as welded Al 6061/5% Sic, welded Al 6061/10% SiCp and welded Al 6061/18% SiCp joints is depicted. A sharp increase in the ultimate tensile strength (UTS) of the welded Al 6061/5% SiCp joint, welded Al 6061/10% SiCp joint welded Al 6061/18% SiCp joint at (120 MPa -135 MPa -195MPa) has been observed as compared to welded Al 6061/5% SiCp, welded 6061/10% Sic at rotation speed 1800 rpm but the UTS of the welded Al 6061/5% SiCp ,welded Al 6061/10% SiCp and welded Al 6061/18% SiCp joint at rotation speed 1000 rpm (100 MPa -115 MPa -165MPa).

It displays a very linear connection of stress-strain to a well-defined yield point. The elastic region is the linear portion of the curve and the slope is the elasticity module or Young's module. As deformation progresses, due to strain hardening, stress rises until it reaches the ultimate strength. Because of Poisson contractions, the cross-sectional region reduces evenly until this stage. The rate of hard work rises as the volume fraction of strengthening rises (and the volume of the matrix decreases). The reduced ductility can be ascribed with a growing quantity of strengthening to the previous onset of void nucleation. As shown in Figure 10, the findings predict an increase in tensile strength as the

reinforcement wt. percent. This can be due to SiCp dispersion that creates obstacles to dislocation movement. A greater pressure must be applied in order to transfer this defect (plastically deforming or yielding the material).

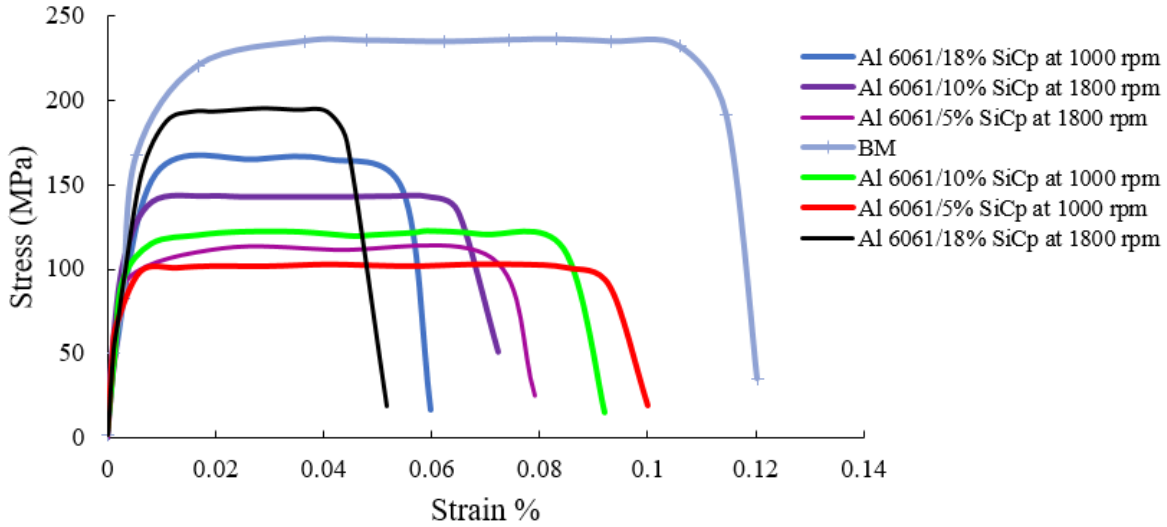


Figure 9. Stress strain curve of welded sample from tensile test for various rotation speed.

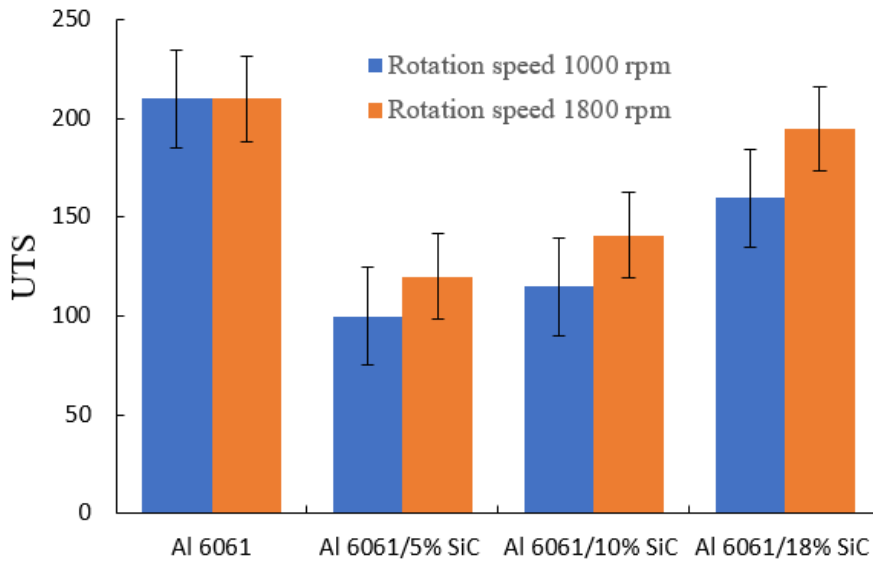


Figure 10. UTS behavior of Al 6061, welded 6061/5% SiCp, welded 6061 10% SiCp and welded Al 6061 18% SiCp (Stander error).

The ultimate tensile strength of the welded joint (195MPa) was observed very near to the UTS of cast composite matrix (300MPa). A joint efficiency of 96.57% was recorded for stir -casting welded joint at rotation speed 1800 rpm. The ultimate tensile strength of the welded joint (165MPa) was observed very near to UTS of cast composite matrix

(200MPa). A joint efficiency of 85.5% was recorded for welded joint at rotation speed 1000 rpm.

At higher tool rotational speed 1800 rpm due to the high heat generation, the plastic flow of material per unit time in the weld zone is increased and reduced the strength of the joint. High rotational 1800 rpm rates enabled the whirling away of particles from the weld zone. Severe clustering of such particles led to the lowering of the tensile strength in the welded stir -casting welded joint as compared to the strength of cast composite matrix [25-29]. The fracture of the FSW weldments occurred near the thermomechanical affected zone region. An appropriate array of friction stir welding variables and flaw-free weld section has been assigned to such a high joint efficiency. The combined effect of appropriate welding variables produced enough frictional heat, optimal stirring action and carrying of stirred plasticized material. A drop-in elongation (%) of the friction stir welded joint has been noticed as shown in Figure 11 due to the disintegration of Sic reinforcing agents and development of fine grains structure in the WZ following to friction stir welding. The outcomes are predicted as the % wt, as shown in Figure 11. The elongation of SiCp rises reduces. This is due to a reduction in ductility as shown above owing to a rise in tensile strength.

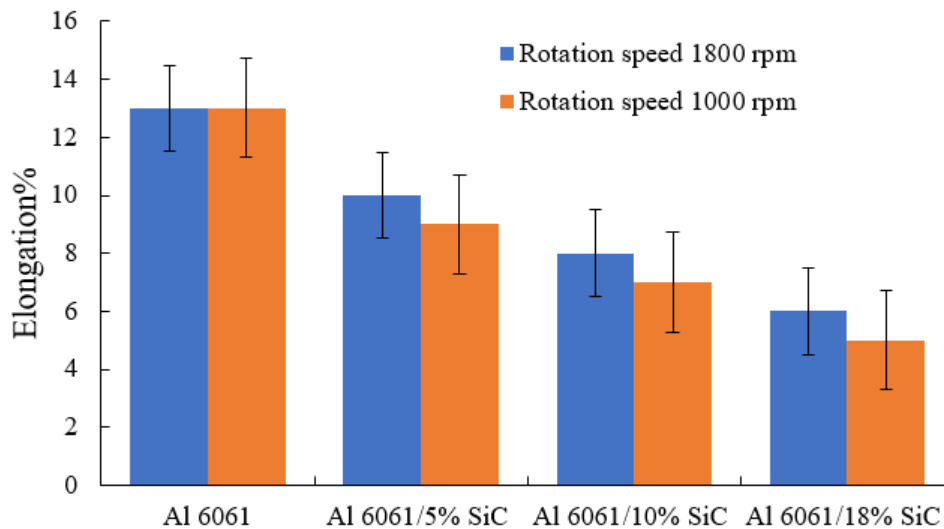


Figure 11. Elongation (%) of Al 6061, welded 6061/5% SiCp, welded Al 6061 10% SiCp and welded Al 6061 18% SiCp (Stander error)

## CONCLUSIONS

Using advanced fixtures and experimental configuration, the joints were successfully friction stir welded for (AMCs). Tensile strength and hardness of welded joints in the nugget zone, heat-affected zone, and thermally heat affected zone. Following the inquiry, the following findings were noted.

1. The FSW of Al 6061 alloy and Al 6061\ SiCp has been successfully produced
2. The FSW welds (ultimate tensile strength) decreases with increase the volume

- fraction of SiCp.
3. The final tensile strength of the welded joint (Al 6061/18 wt. percent) was 195 MPa at rotation velocity 1800 rpm, resulting in 165 MPa at rotation velocity 1000 rpm being the ultimate tensile strength of the welded joint (Al 6061/18 wt. percent), which was very near to the strength of the as-cast composite matrix.
  4. Due to elevated heat generation at rotational speed of 1800 rpm, the ultimate tensile strength of the welded joint was reduced by 4 % compared to the ultimate tensile strength of the base composite matrix.
  5. The grain structure in the area impacted by heat, which was not mechanically troubled by friction stir welding, is comparable to that of the base metal, grains in the area impacted by base metal and heat contain a comparatively small density of dislocation.
  6. A drop-in elongation (%) at Al 6061/18 wt. % of the FS welded joint was noticed due to the disintegration of SiCp reinforcing agents and development of fine grains structure in the weld zone following to FS welding.

## **REFERENCES**

- [1] Davis JR. ASM Specialty Handbook: Aluminum and aluminum alloys, ASM International, Inc; 1993.
- [2] Ghosh S, Saha P. Crack and wear behavior of Sic particulate reinforced aluminum-based metal matrix composite fabricated by direct metal laser sintering process. *Materials and Design*. 2011; 32:39-145.
- [3] Foltz JV, Blackmon. Metal-matrix composites. In ASM International, *Metals Handbook, Properties and Selection: Nonferrous Alloys and Special-Purpose, Materials*. 1990;10:903-912.
- [4] Scudino S, Liu G, Prashanth KG, Bartusch B, Surreddi KB, Murty BS, Eckert J. Mechanical properties of Al-based metal matrix composites reinforced with Zr based glassy particles produced by powder metallurgy. *Acta Materialia*. 2009;57:2029-2039.
- [5] Ross M. Ceramic and metal matrix composites: routes and properties. *Journal of Materials Processing Technology*. 2006;175:364-375.
- [6] Prater T. Solid-state joining of metal matrix composites: a survey of challenges and potential solutions. *Materials and Manufacturing Processes*. 2011;26(4): 636– 648.
- [7] Storjohann D, Barabash OM, Babu SS, David SA, Sklad PS, Bloom EE. Fusion and friction stir welding of aluminum–metal–matrix composites. *Metal Mater Trans A*. 2005;36:3237– 3247.
- [8] Guo J, Gougeon P, Chen XG. Study on laser welding of AA1100-16 vol.% B4C metal–matrix composites. *Composites Part B*. 2012; 43(5):2400–2408.
- [9] Xi-He W, Ji-tai N, Kang GS, Le-jun W, Feng CD. Investigation on TIG welding of SiCp-reinforced aluminum–matrix composite using mixed shielding gas and Al–Si filler. *Material Science and Engineering: A*. 2009; 499(1-2):106–110.
- [10] Wang SG, Ji XH, Zhao XQ, Dong NN. Interfacial characteristics of electron beam welding joints of SiCp/Al composites. *Material Science and Technology*. 2011;27:60-64.

- [11] Cam G. Friction stir welded structural materials: beyond Al-alloys. *International Materials Reviews*. 2011;56:1-48.
- [12] Threadgill PL, Leonard AJ, Shercliff HR, Withers PJ. Friction stir welding of aluminum alloys. *International Materials Reviews*. 2009;54:49–93.
- [13] Chen XG, Da Silva M, Gougeon P, St-Georges L. Microstructure and mechanical properties of friction stir welded AA6063–B4C metal matrix composites. *Material Science and Engineering: A*. 2009;518:174–184.
- [14] Vijay SJ, Murugan N. Influence of tool pin profile on the metallurgical and mechanical properties of friction stir welded Al–10 wt.% TiB<sub>2</sub> metal matrix composite. *Materials & Design*. 2010;31(7):3585-3589.
- [15] Nami H, Adgi H, Sharifitabar M, Shamabadi H. Microstructure and mechanical properties of friction stir welded Al/Mg<sub>2</sub>Si metal matrix cast composite. *Materials & Design*. 2010;32:976–983.
- [16] Gopalakrishnan S, Murugan N. Prediction of tensile strength of friction stir welded aluminum matrix TiCp particulate reinforced composite. *Materials & Design*. 2011; 32(1):462-467.
- [17] Kalaiselvan K, Dinaharan I, Murugan N. Characterization of friction stir welded boron carbide particulate reinforced AA6061 aluminum alloy stir cast composite. *Materials & Design*. 2014;55:176-182.
- [18] Hasan MM, Ishak M, Rejab MRM. A simplified design of clamping system and fixtures for friction stir welding of aluminum alloys. *Journal of Mechanical Engineering and Sciences*. 2015;9:1628-1639.
- [19] Sabry I, El-Kassas AM. Comparative Study on different tool geometries in friction stirred aluminum welds using response surface methodology. In: 4th International Conference on Welding and Failure Analysis of Engineering Materials, Aswan, Egypt November 19-22, 2018.
- [20] Wang D, Xiao BL, Wang QZ, Ma ZY. Friction stir welding of SiCp/2009Al composite plate. *Materials and Design*. 2013;47:243–247.
- [21] Bahrami M, Helmi N, Dehghani K, Givi MKB. Exploring the effects of SiC reinforcement incorporation on mechanical properties of friction stir welded 7075 aluminum alloy: fatigue life, impact energy, tensile strength. *Materials Science and Engineering: A*. 2014;595:173-178.
- [22] Midling OT, Material flow behavior & microstructural integrity of friction stir butt weldments. In: 1st International Conference on Aluminum Alloys, September 1994:451–458.
- [23] Guo J, Amira S, Gougeon P, Chen XG. Effect of the surface preparation techniques on the EBSD analysis of a friction stir welded AA1100-B4C metal matrix composite. *Materials Characterization*. 2011; 62(9):865–877.
- [24] Guo J, Amira S, Gougeon P, Chen XG. Joining of AA1100–16 vol.-%B4C metal matrix composite using laser welding and friction stir welding. *Journal Canadian Metallurgical Quarterly*. 2012 ; 51(3) :277-283
- [25] Azimzadega T, Serajzadeh S. An investigation into microstructures and mechanical properties of AA7075-T6 during friction stir welding at relatively high rotational speeds. *Journal of Materials Engineering and Performance*. 2010; 19(9):1256-1263.
- [26] Sabry I, El-Kassas AM, Mourad AHI, Thekkuden DK, Qudeiri JK. Friction stir welding of T-joints: Experimental and Statistical analysis, *Journal of Manufacturing*

- and Materials Processing. 2019; 3(2) :1-23.
- [27] El-Kady O, Fathy A. Effect of SiC particle size on the physical and mechanical properties of extruded Al matrix nanocomposites, *Materials and Design*, February 2014; 54:348-353.
- [28] Narinder kaushik, Sandeep Singhal, Rajesh, Pardeep Gahlot, B N Tripathi. Experimental investigations of friction stir welded AA6063 aluminum matrix composite. *Journal of Mechanical Engineering and Sciences*. 2018;12(4) :4127-4410.
- [29] Osman N, Sajuri Z, Omar MZ. Multi-pass friction stirred clad welding of dissimilar joined AA6061 aluminium alloy and brass. *Journal of Mechanical Engineering and Sciences*. 2018; 12(4) : 4285-4299